JOURNAL OF ENGINEERING SCIENCES

Volume 11, Issue 2 (2024)

Kondus V., Ciszak O., Zhukov A., Mushtai M., Polkovnychenko V., Krugliak A. (2024). Development of a self-cleaning mechanism for torque-flow pumps. Journal of Engineering Sciences (Ukraine), Vol. 11(2), pp. F17–F26. https://doi.org/10.21272/jes.2024.11(2).f3

Development of a Self-Cleaning Mechanism for Torque-Flow Pumps

Kondus V.[1,2*][0000-0003-3116-7455], Ciszak O.[3][0000-0002-0877-5797], Zhukov A.[1][0009-0000-6956-6553], Mushtai M.[1][0009-0006-3102-2351], Polkovnychenko V.[1][0009-0000-4030-535X], Krugliak A.[1][0009-0006-0279-9145]

[1] Sumy State University, 116, Kharkivska St., 40007, Sumy, Ukraine;
[2] Sumy Machine-Building Cluster of Energy Equipment, 116, Kharkivska St., 40007, Sumy, Ukraine;
[3] Poznan University of Technology, 5, Marii Skłodowskiej-Curie Sq., 60-965, Poznan, Poland

Article info:

Submitted:	August 2, 2024
Received in revised form:	November 15, 2024
Accepted for publication:	November 18, 2024
Available online:	November 21, 2024

***Corresponding email:**
v.kondus@pgm.sumdu.edu.ua

Abstract. The design of reliable and durable pumping units is consistent with the achievement of a number of the United Nations' sustainable development goals (SDG), in particular, "Clean water and proper sanitation" (SDG 6), "Affordable and clean energy" (SDG 7), and "Industry, innovation and infrastructure" (SDG 9). Notably, the use of torque-flow pumps is associated with the need to transport liquids of various types. Such an operating process can cause clogging of the flowing part of the pump (primarily the impeller) by pumping products, mainly wet wipes, solids, and inclusions. As a result of scientific research, an effective self-cleaning mechanism for the torque-flow pump was developed, which was the primary goal. The authors proved that the flow of actual fluid in the interblade channels of the impeller is characterized by an uneven distribution of absolute pressure and relative speed, which is a prerequisite for forming an uneven pulsating nature of motion (the key hypothesis of the study). To implement the proposed hypothesis, an impeller with uniform and non-uniform distribution of blades was developed, and the movement of actual fluid flow in their interblade channels was considered. As a result of the research, it was established that in the expanded interblade channels, there is a pulsation of the absolute (total) pressure value, which is more than 2 times higher than the indicator of an impeller with a uniform distribution of blades. This creates prerequisites for self-cleaning of the developed impeller of the torque-flow pump.

Keywords: energy efficiency, vibration reliability, durability, UN SDGs, process innovation, life cycle cost.

1 Introduction

Currently, there is a rapid increase in the cost of energy resources, particularly electricity [1]. This is primarily due to logistical problems and growing energy consumption in the world [2]. Remarkably, the pumping equipment itself is one of the leading energy consumers in various industries, particularly when transporting liquids with inclusions [3].

Considering the implementation of the United Nations' sustainable development goals (SDG) [4], reducing energy consumption by pumping equipment is a key indicator of achieving "Affordable and clean energy" (SDG 7). The design of reliable and durable pumping units [5] is closely related to the achievement of "Industry, innovation and infrastructure" (SDG 9) and "clean water and proper sanitation" (SDG 6). It also helps to increase the competitiveness of the manufacturer of such equipment. For example, even a slight decrease in weight and size indicators leads to a decrease in the cost price and, therefore, in the market's competitiveness [6].

In turn, the reduction of weight and size indicators allows the use of higher-quality (but more expensive) construction materials and technologies that reduce energy consumption [7] and increase the reliability of the equipment [8].

It should be noted that torque-flow pumps (Figure 1), the operating process considered in this article, specialize in transporting liquids with various inclusions [9], such as solid, fibrous, and abrasive.

A typical example of the operating fluids pumped by pumps of this type are suspensions, syrups, and liquids containing household waste [10], mainly wet wipes, hygiene products, and so on.

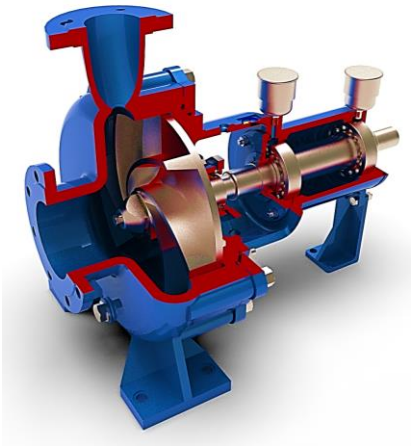

Figure 1 – structural view of the torque-flow pump of the "Turo" type

The transportation of such operating fluids is accompanied by clogging the flowing parts of the pumps. This leads to decreased operational performance, particularly energy efficiency [11]. Therefore, the operation of torque-flow pumps requires the creation of self-cleaning mechanisms [12].

2 Literature Review

Increasing the technical level (an integral energy efficiency component) of hydraulic machines is generally achieved according to the final assessment criterion at the design stage [13].

Thus, increasing the energy efficiency of pumps of various types is achieved by deep modification of the design of the elements of the flowing part, particularly the impeller [14].

In research [15], the principle of operation of torque-flow pumps is considered, and a methodical approach for evaluating the energy efficiency of its operating process is proposed. In order to increase it, the article [16] proposed an improved design of the diverter device of the pump. However, such a design greatly complicates its manufacture and, as a result, the final cost [17].

At the same time, the modification of the operating process in order to increase the energy efficiency of torque-flow pumps is possible by changing the operating body, which is the pump's impeller [18]. In particular, it was proved that the replacement of standard impellers with radial blades for impellers with curved blades made it possible to increase the energy efficiency of the pump by 3–5 % [19]. It should be noted that such a change in the design scheme at the inlet to the impeller will not lead to cavitation phenomena [20], even without the need to develop additional precautionary measures [21].

Increasing the energy efficiency of torque-flow pumps can be achieved by lengthening part of the blades to the free chamber of the pump [22], as well as creating additional winglets on the edges of the impeller's blades [23]. The specified methods will generally ensure a steady flow before and after the pump in the line without additional hydraulic energy losses due to vortex formation, which is essential for the pumps' operational quality [24].

In order to regulate the operating parameters of torque-flow pumps, a wide variety of design schemes have been developed. Thus, in [25], the effect of the design elements of the blade on the pump's operating parameters was considered. Similar studies were carried out for torque-flow pumps of the "Seka" type, characterized by the impeller's protrusion into the pump's free chamber [26].

Notably, the design features of the inlet part to the impeller of torque-flow pumps provide high resistance to the occurrence of cavitation phenomena. As a result, such pumps do not require separate anti-cavitation devices [27], significantly simplifying the submersible device's design compared to centrifugal pumps [28].

However, insufficient attention is paid to pumping equipment's energy efficiency and reliability in the long-term transportation of contaminated liquids and liquids with inclusions [29].

The article [30] researched the operation of centrifugal pumps based on the damping effects of flow parts with slotted seals. Notably, critical factors in reducing the reliability of such pumps are the rapid failure of bearings and seals [31]. Simultaneously, bearingless pumps can operate due to the centering of the rotor in the sealing unit. In this case, the pump's reliability depends on the sealing devices' reliability [32, 33].

Long-term reliable and energy-efficient operation of torque-flow pumps when pumping contaminated liquids is an unexplored problem. This is explained by the complexity of the operating process using a heterogeneous medium and the unpredictability of the quantitative content and structure of the multiphase medium in such operating processes. However, torque-flow pumps are usually operated under such conditions. Thus, their operating process requires parameter indicators during bench research when transporting pure liquids and maintaining such indicators in multiphase media. This requires the development of effective methods of self-cleaning during the operation of pumping equipment.

Because of this, the study aims to develop and research an effective method of self-cleaning of torque-flow pumps during their operation to maintain high parameters (pressure, energy efficiency, and cavitation).

In order to ensure the set aim, the following tasks were stated for the research: determination of the theoretical mechanisms of self-cleaning of the flowing part of the torque-flow pump, formation of the research hypothesis, development of a constructive implementation of flowing part elements with a self-cleaning mechanism; conducting experimental studies to confirm the proposed hypothesis; analysis of experimental research results.

3 Research Methodology

3.1 Design features of torque-flow pumps

During the operation of torque-flow pumps, the pump's operating peculiarities should be considered (Figure 2).

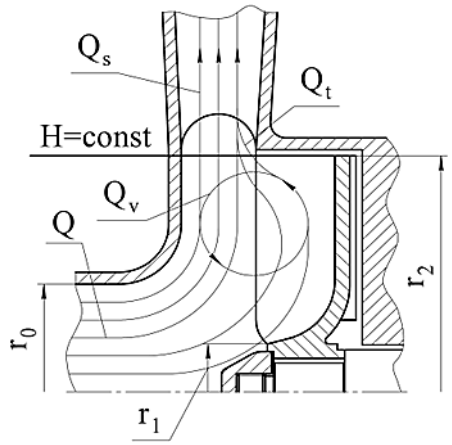

Figure 2 – Features of the operating process of torque-flow pumps: Q – supply of liquid to the pump; Q_v – vortex operating process; Q_t – blade operating process; Q_s – the flowing stream

They consist of the simultaneous presence of both a blade operating process (traditional for dynamic type pumps) and a vortex operating process (more common among vortex hydraulic machines) [34].

During the pump operation, the flow of the working medium is divided into two main parts. The first part directly receives energy due to force interaction with the impeller blades. The second part forms a vortex motion (the so-called toroidal vortex). This part of the working medium receives energy from force interaction with the blades and transmits the flowing stream, which is not in direct contact with the impeller blades. Thus, a complex two-stage operating process is formed in the flowing part of the torque-flow pump. Such an unconventional energy transfer route must be considered when developing, designing, and operating pumps of this type.

3.2 The rationale for creating a self-cleaning mechanism for free-vortex pumps

Usually, the design of flowing parts is performed based on L. Euler's jet theory. According to it, the graph of relative speed (and, accordingly, pressure) is evenly distributed along the interblade channel of the impeller (Figure 3a).

Considering the real fluid flow (Figure 3b), the distribution of the relative velocity in the interblade channels of the impeller is uneven. At the same time, its value is greater near the rear side of the blade and less near the operating side. Accordingly, the pressure created in the interblade channels is also uneven. It is larger near the operating side of the blade and smaller near its back side.

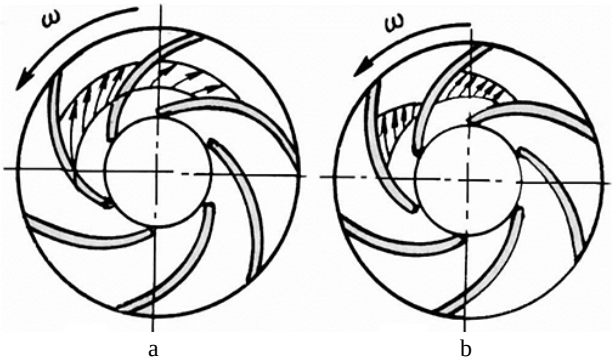

Figure 3 – The design schemes of the relative velocity distribution in the interblade channel of the impeller according to Euler's jet theory (a) and for the actual liquid flow (b)

This effect can be neglected when designing centrifugal pumps since the fluid movement in the impeller, in this case, is directed radially. Thus, in such cases, there is no intensive mixing of liquid layers in the axial direction at the exit from the impeller.

During the operation of the torque-flow pump, the liquid outlets from the interblade channels of the impeller (Figure 4) mainly in the axial direction. Therefore, the influence of the uniformity of the flow through the channels cannot be neglected.

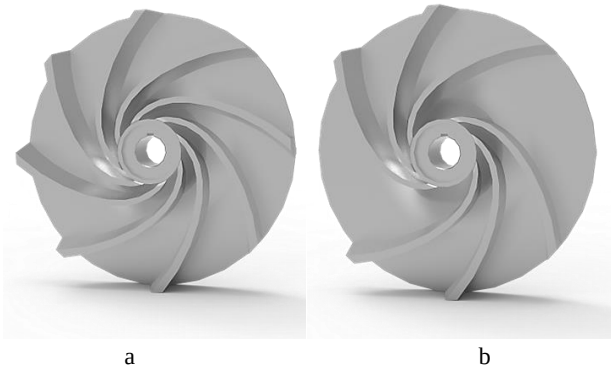

Figure 4 – Impeller's designs for a torque-flow pump with uniform (a) and uneven (b) blade distribution

Simultaneously, if the blades are evenly spaced, the pressure distribution at the outlet of the interblade channels of the liquid will be more or less cyclical, leading to a steady movement of the liquid. In turn, this will not cause significant pressure pulsations in the free chamber of the pump.

This article proposes that a self-cleaning mechanism be created due to the pulsation of the flow at the outlet of the impeller. It is proposed to do this by unevenly arranging the blades (2 channels are doubled, Figure 4b). On the one hand, this design will allow for static and dynamic balancing of the rotor [35]. On the other hand, the relative velocity (and, accordingly, the pressure) at the exit from the interblade channels will be uneven. This will create the prerequisites for pulsatile pushing effects on the pumped media (the key hypothesis of the study).

3.3 Methodology of conducting numerical simulations for the operating process

In order to reduce time and investment costs and present the results more clearly, numerical research using the ANSYS CFX software was used during the research. This software has proven itself as a reliable way of modeling hydraulic processes [36], mainly when modeling dynamic [37] and torque-flow [38] pumps. The difference between numerical modeling and physical experiment results does not exceed 5 %. Therefore, this software product is suitable for solving the research problem.

The torque-flow pump was chosen as the research object. The operating parameters are given in Table 1.

Table 1 – Operating parameters

Parameter	Unit	Value
Head	m	60
Flow rate	m^3/h	125
Rotational frequency	rpm	1500
Efficiency	%	40

The obtained results will be analyzed in graphic and numerical forms. The graphic form consists of studying the nature of the flow movement inside the interblade channels at 5 mm from the edge of the blade (Figure 5a), in the middle of the interblade channel (Figure 5b), and at 5 mm from the impeller disk wall (Figure 5c).

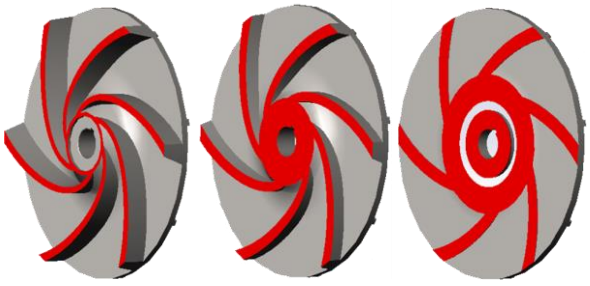

a b c

Figure 5 – Planes of presentation of research results:
a – at 5 mm from the edge of the blade;
b – in the middle of the interblade channel of the impeller;
c – at 5 mm from the surface of the impeller disk

This is explained by the need to distort the research results due to the influence of the wall layer of the operating fluid [39]. The numerical form allows authors to present the obtained results as graphical dependences of pressure on the position of the studied jet in the interblade channel of the impeller.

The total pressure at a point can be determined according to the Bernoulli's equation:

$$p_{tot} = p_{stat} + \frac{1}{2}\rho v_{rel}^2, \quad (1)$$

where p_{stat} – static pressure at this point, Pa; ρ – density of the operating fluid, kg/m^3; v_{rel} – relative velocity in the rotating frame of reference at this point, m/s.

In turn, the relative velocity in the rotating frame of reference can be determined as follows:

$$\vec{v}_{rel} = \vec{v}_{stn} - \vec{\omega} \times \vec{R}, \quad (2)$$

where v_{stn} – static velocity in the stationary frame of reference, m/s; ω – angular velocity, rad/s; R – local radius vector, m.

The ANSYS CFX software, based on the numerical solution of the fundamental laws of hydromechanics, was used during the research.

Water with a temperature of 20 °C and a turbulent mode of movement was chosen as the operating medium. The standard "k–ε" turbulence model was used to close the Reynolds equations, proving itself well in the above studies.

The value of the variable y+, which characterizes the thickening of the grid near the walls, was within $20 < y^+ < 100$.

A stator (housing and free chamber, inlet and outlet devices) element and a rotor (impeller) element were selected. Standard unstructured grids created in the ICEM CFD environment are selected as walls. The total number of grid cells is about 1.5 million (stator – $1.03 \cdot 10^6$ cells, rotor – $0.49 \cdot 10^6$ cells). Calculation grids include local thickenings near the walls, made according to the exponential law in the form of prismatic layers with the following parameters: initial height – 0.05 mm; height ratio – 1.5; number of layers – 7; the total height – 1.6 mm.

The grid convergence quality of standard unstructured grids was no less than 0.31 for the rotor element (impeller) and 0.36 – for the stator element.

The research was carried out to converge the main parameters to $1 \cdot 10^{-4}$. The convergence of pressure, power, and energy efficiency was monitored separately, considering the achievement of a discrepancy of no more than 0.05 in amplitude according to the last 20 iterations.

4 Results

As a result of the research, the pressure distribution in the impeller with a uniform and uneven distribution of blades was obtained at 5 mm from the blade's edge, in the middle of the interblade channel of the impeller, and at 5 mm from the surface of the impeller disk (Figure 6).

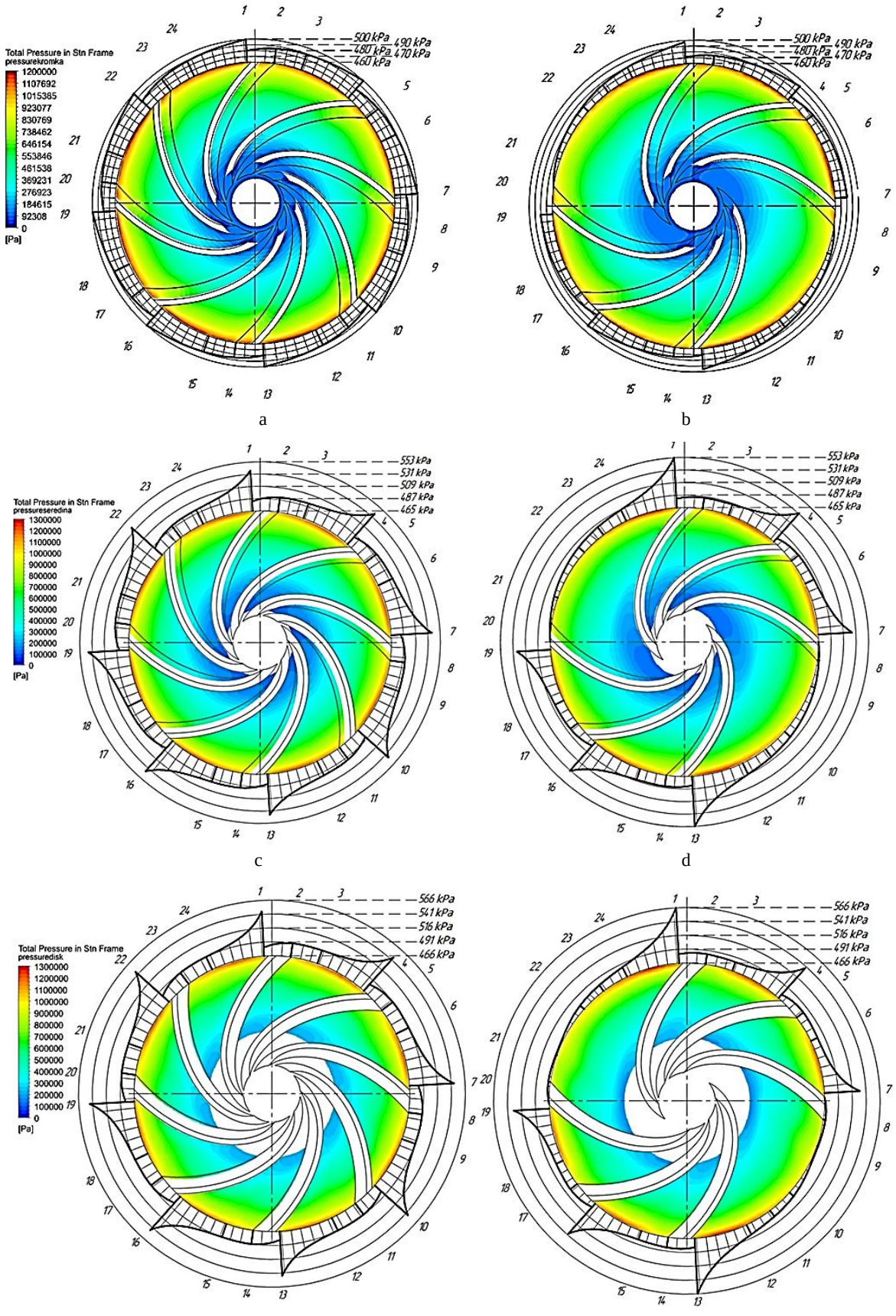

Figure 6 – Pressure distribution in the impeller with uniform (a, c, e) and uneven (b, d, f) distribution of blades: a, b – at 5 mm from the blade's edge; c, d – in the middle of the interblade channel of the impeller; e, f – at 5 mm from the surface of the impeller disk

Simultaneously, the obtained results are given in the form of fill by the value of absolute (total) pressure, in which smaller values of absolute pressure correspond to more "cold" colors, and to higher values of absolute pressure – more "hot" colors, as well as in the form of a graph with a scale that describes the change absolute pressure in the interblade channels of the torque-flow pump impeller.

To ensure an adequate analysis of the obtained results, the pressure graph is divided into 24 sectors with a step of 15°. This made it possible to reproduce the results in graphs as accurately as possible.

The results prove the non-uniformity of the pressure distribution along the interblade channels of the impeller (Tables 2–4). Moreover, higher absolute pressure values are observed near the operating side of the blade, and smaller values are observed near the rear side of the blade.

In turn, the value of the absolute pressure increases in the direction of the flow of the operating fluid from the center to the periphery. For an impeller with a uniform distribution of blades, a cyclic distribution of the absolute pressure plot is observed at 5 mm from the edge of the blade (Figure 6a). This pressure distribution has a more pronounced character in the middle of the interblade channel of the impeller (Figure 6c) and is especially pronounced at 5 mm from the surface of the impeller disk (Figure 6e).

In turn, for an impeller with an uneven distribution of blades at 5 mm from the edge of the blade (Figure 6b), a non-cyclic distribution of the absolute pressure plot is observed. Moreover, this non-cyclic nature of the distribution of the absolute pressure plot is more pronounced in the direction from the edge of the blades of the impeller to the surface of its disk, in particular in the middle of the interblade channel of the impeller (Figur 6d) and especially at 5 mm from the surface of the impeller disk (Figure 6f).

Thus, the indicated nature of the movement of the operating fluid in the impeller with a uniform distribution of blades creates prerequisites for its stable movement without the formation of pulsation phenomena. In turn, the nature of the movement of the operating fluid in the impeller with an uneven distribution of blades of the specified design creates prerequisites for the occurrence of pulsation phenomena in the direction from the disk to the edges of the impeller blades.

The movement of fluid in such an impeller will have an unsteady character. This creates the prerequisites for creating a self-cleaning effect due to the unstable pulsating movement of the working fluid in different interblade channels of such an impeller.

Table 2 – Pressure distributions at 5 mm from the blade's edge (Figures 6 a–b)

Line	Uniform distribution	Uneven distribution	Pressure difference	
	kPa	kPa	kPa	%
1'	480	470	10	2.1
2	486	473	13	2.7
3	488	477	11	2.3
4	500	488	12	2.5
4'	480	467	13	2.8
5	486	471	15	3.2
6	488	473	15	3.2
7	500	479	21	4.4
7'	480	460	20	4.3
8	486	460	26	5.7
9	488	463	25	5.4
10	500	470	30	6.4
10'	480	470	10	2.1
11	486	473	13	2.7
12	488	478	10	2.1
13	500	496	4	0.8
13'	480	472	8	1.7
14	486	474	12	2.5
15	488	479	9	1.9
16	500	490	10	2.0
16'	480	468	12	2.6
17	486	472	14	3.0
18	488	474	14	3.0
19	500	491	9	1.8
19'	480	460	20	4.3
20	486	460	26	5.7
21	488	465	23	4.9
22	500	472	28	5.9
22'	480	472	8	1.7
23	486	474	12	2.5
24	488	479	9	1.9
1	500	498	2	0.4

Table 3 – Pressure distributions in the middle of the interblade channel (Figures 6 c–d)

Line	Uniform distribution	Uneven distribution	Pressure difference	
	kPa	kPa	kPa	%
1'	485	482	3	0.6
2	493	484	9	1.9
3	495	485	10	2.1
4	535	533	2	0.4
4'	485	476	9	1.9
5	493	480	13	2.7
6	495	482	13	2.7
7	537	525	12	2.3
7'	485	465	20	4.3
8	493	467	26	5.6
9	495	469	26	5.5
10	535	481	54	11.2
10'	485	481	4	0.8
11	493	484	9	1.9
12	495	486	9	1.9
13	535	553	-18	–3.3
13'	485	484	1	0.2
14	493	485	8	1.6
15	495	486	9	1.9
16	535	532	3	0.6
16'	485	476	9	1.9
17	493	480	13	2.7
18	495	482	13	2.7
19	535	525	10	1.9
19'	485	465	20	4.3
20	493	467	26	5.6

Line	Uniform distribution	Uneven distribution	Pressure difference	
	kPa	kPa	kPa	%
21	495	469	26	5.5
22	535	481	54	11.2
22’	485	481	4	0.8
23	493	484	9	1.9
24	495	486	9	1.9
1	535	553	–18	–3.3

Table 4 – Pressure distributions at 5 mm from the surface of the impeller disk (Figures 6 e–f)

Line	Uniform distribution	Uneven distribution	Pressure difference	
	kPa	kPa	kPa	%
1’	488	485	3	0.6
2	492	485	7	1.4
3	494	483	11	2.3
4	543	538	5	0.9
4’	488	470	18	3.8
5	492	481	11	2.3
6	494	477	17	3.6
7	543	530	13	2.5
7’	488	466	22	4.7
8	492	468	24	5.1
9	494	467	27	5.8
10	543	471	72	15.3
10’	488	471	17	3.6
11	492	474	18	3.8
12	494	480	14	2.9
13	543	566	–23	–4.1
13’	488	485	3	0.6
14	492	485	7	1.4
15	494	483	11	2.3
16	543	538	5	0.9
16’	488	470	18	3.8
17	492	481	11	2.3
18	494	477	17	3.6
19	543	530	13	2.5
19’	488	466	22	4.7
20	492	468	24	5.1
21	494	467	27	5.8
22	543	471	72	15.3
22’	488	471	17	3.6
23	492	474	18	3.8
24	494	480	14	2.9
1	543	566	-23	–4.1

5 Discussion

A graphic image (plot) of the pressure distribution in the interblade channels of the impeller with a uniform distribution of the blades proves the uniform distribution of the total pressure in all the interblade channels of the impeller. This confirms the absence of significant flow pulsations in the interblade channels of such an impeller, which is promising when the pump pumps clean liquids that do not contain sediment [16]. However, this design of the flowing part of the pump is prone to contamination and the formation of deposits when pumping liquids with inclusions (e.g., suspensions, sewage masses).

When using such impellers, the lowest absolute pressure is observed in the area near the rear side of the blades. This value is at least 480 kPa at 5 mm from the edge of the blade (Figure 6a), at least 485 kPa in the middle of the interblade channel of the impeller (Figure 6c), at least 490 kPa at 5 mm from the surface of the impeller disk (lines 2, 5, 8, 11, 14, 17, 20, and 23).

In turn, the highest absolute pressure is observed in the area near the working side of the blades. This value is no more than 500 kPa at 5 mm from the edge of the blade (Figure 6a), no more than 535 kPa in the middle of the interblade channel of the impeller (Figure 6c), and no more than 543 kPa at 5 mm from the surface of the impeller disk (lines 1, 4, 7, 10, 13, 16, 19, and 22).

Simultaneously, no significant changes in absolute pressure are observed in most sections of the interblade channels (1–3, 4–6, 7–9, 10–12, 13–15, 16–18, and 22–24). Its values are approximately 490 kPa at 5 mm from the edge of the blade (Figure 6a), 491 kPa in the middle of the interblade channel of the impeller (Figure 6c), and 492 kPa – at 5 mm from the disk’s surface.

Thus, in most areas of such an impeller, a stable value of the absolute pressure at the outlet of the impeller is approximately equal to 491 kPa [23].

At the same time, the absolute pressure difference between the most significant and smallest values does not exceed 20 kPa at 5 mm from the edge of the blade (Figure 6a), 50 kPa in the middle of the interblade channel of the impeller (Figure 6c), and 53 kPa – at 5 mm from the surface of the impeller disk (Figure 6e). The flow pattern is significantly different when using an impeller with an uneven distribution of blades.

When using such impellers, the lowest absolute pressure is observed in the area near the back side of the blades. This value is at least 470 kPa at 5 mm from the edge of the blade (Figure 6a), at least 475 kPa in the middle of the interblade channel of the impeller (Figure 6c), and at least 485 kPa – at 5 mm from the surface of the impeller disk (lines 2, 5, 8, 14, 17, and 20).

In turn, the highest absolute pressure is observed in the area near the operating side of the blades. This value is no more than 497 kPa at 5 mm from the edge of the blade (Figure 6a), no more than 530 kPa in the middle of the interblade channel of the impeller (Figure 6c), and no more than 538 kPa at 5 mm from the surface of the impeller disk (lines 1, 4, 7, 13, 16, and 19).

Simultaneously, no significant changes in absolute pressure are observed in most interblade channel sections (1–3, 4–6, 13–15, and 16–18). Its value is approximately 490 kPa at 5 mm from the edge of the blade (Figure 6a), 491 kPa in the middle of the interblade channel of the impeller (Figure 6c), 492 kPa at 5 mm from the surface of the impeller disk.

At the same time, there is an increase in the gap between the most significant and smallest values of absolute pressure on the interblade channels of the impeller, which are increased by the coverage angle. Thus, the highest absolute pressure is observed in the area near the operating side of the blades. This value is no more than 500 kPa at 5 mm from the edge of the blade (Figure 6a), no more than 553 kPa in the middle of the interblade channel of the impeller (Figure 6c), no more than 566 kPa at 5 mm from the surface of the impeller disk (lines 1, 13). Simultaneously, a reduced absolute pressure value (at least 455 kPa) is observed over a wide range of the coverage

angle (lines 8–12, 20–24). Thus, the absolute pressure difference in such expanded interblade channels is up to 111 kPa (more than 2 times greater than that of an impeller with a uniform distribution of blades) with a sharp increase in the direction from the rear to the working side of the blade.

This creates a sharp pulsating effect on the change in absolute pressure when using an impeller with an uneven distribution of blades and creates prerequisites for self-cleaning the developed impeller [34].

6 Conclusions

As a result of scientific research, an effective self-cleaning mechanism for the torque-flow pump was created. This is ensured by creating prerequisites for pulsation processes in the interblade channels of the impeller with an uneven distribution of blades.

First, the theoretical mechanisms of self-cleaning were considered to ensure the goal. The authors found that, unlike Euler's jet theory, the flow of actual fluid in the interblade channels of the impeller is characterized by an uneven distribution of absolute pressure and relative velocity. At the same time, an increased absolute (total) pressure is observed near the operating side of the impeller blades, while it is lower on the back (rear) side. This creates prerequisites for forming an uneven pulsating nature of the movement of actual fluid in interblade channels when using an impeller with an uneven distribution of blades, which was the central hypothesis.

Second, an impeller with a uniform and uneven distribution of blades was developed to implement the proposed hypothesis. Simultaneously, in the first case, 8 blades were made, and in the second, 6 blades were made (considering two symmetrically located interblade channels that are twice as large in coverage angle).

The experimental study was also performed using numerical data from ANSYS CFX software. The reviewed literary sources allow us to assert the high convergence of research results with experimental data obtained during parametric tests of the pump using a hydraulic test bench. This research method allows for the analysis of the results.

Finally, based on the results of the research, it was determined that when using an impeller with a uniform distribution of blades, the absolute pressure value changes in the direction of movement from the rear side to the operating side of the blade of the impeller cyclically, and its amplitude does not exceed 53 kPa. However, when using an impeller with a uniform distribution of blades, the absolute pressure value in the standard interblade channels changes in the direction of movement from the rear side to the operating side of the blade of the impeller cyclically, and its amplitude does not exceed 53 kPa. However, in the expanded interblade channels (lines 8-12, 20-24), there is a pulsation of pressures in the range of up to 111 kPa (more than 2 times the indicator of an impeller with a uniform distribution of blades) with a sharp increase in the direction from the rear to the operating side of the blades. A sharp pulsating effect on the change in absolute pressure creates the prerequisites for self-cleaning.

Thus, the research is fundamental to developing torque-flow pumps with a self-cleaning effect and studying their operating process. The presented findings will be further used to expand the application of torque-flow pumps by developing new ones.

Acknowledgment

The study was conducted within the framework of the R&D project "Development of design solutions and layout schemes of a parametric series of high-speed energy-efficient well pumps for the needs of enterprises in the field of critical infrastructure" (No. 2022.01/ 0096) of the National Research Foundation of Ukraine for the possibility of project implementation. The authors also appreciate the support of the Public Union "Sumy Machine-Building Cluster of Energy Efficiency".

References

1. Ren, Z., Sun, M., Zhang, J., Wang, X., Huang, Z., Xu, J., Huang, C. (2023). Start-up strategy of mixed-flow pump system with impulse operation. *Ocean Engineering*, Vol. 277, 114058. https://doi.org/10.1016/j.oceaneng.2023.114058
2. Danylyshyn, V., Koval, M. (2022). Development of alternative energy in the world and Ukraine. *Machinery & Energetics*, Vol. 13(2), pp. 50–61. https://doi.org/10.31548/machenergy.13(2).2022.50-61
3. Tverdokhleb, I., Semenov, A., Ivanyushin, A., Niemtsev, O., Rudenko, A. (2014). Creating a standard size range as one of the factors reducing production time of modern pumping equipment. *Applied Mechanics and Materials*, Vol. 630, pp. 137–142. https://doi.org/10.4028/www.scientific.net/AMM.630.137
4. United Nations. General Assembly Resolution A/RES/70/1. Transforming Our World, the 2030 Agenda for Sustainable Development. (2015). Available online: https://www.un.org/ (accessed on July 29, 2024).
5. Ahmed, A.A., Moharam, B.A., Rashad, E.E. (2022). Improving energy efficiency and economics of motor-pump-system using electric variable-speed drives for automatic transition of working points. *Computers & Electrical Engineering*, Vol. 97, 107607. https://doi.org/10.1016/j.compeleceng.2021.107607
6. Antonenko, S., Sapozhnikov, S., Kondus, V., Chernobrova, A., Mandryka, A. (2021). Creation a universal technique of predicting performance curves for small-sized centrifugal stages of well oil pump units. *Journal of Physics: Conference series*, Vol. 1741, 012011. https://doi.org/10.1088/1742-6596/1741/1/012011
7. Shuiguang, T., Hang, Z., Huiqin, L., Yue, Y., Jinfu, L., Feiyun, C. (2020). Multi-objective optimization of multistage centrifugal pump based on surrogate model. *Fluids*, Vol. 142(1), 011101. https://doi.org/10.1115/1.4043775

8. Kumar, J., Gopi, S., Amirthagadeswaran, K. (2023). Redesigning and numerical simulation of gating system to reduce cold shut defect in submersible pump part castings. *Proceedings of the Institution of Mechanical Engineers, Part E: Journal of Process Mechanical Engineering*, Vol. 237(3), pp. 971–981. https://doi.org/10.1177/09544089221142185
9. Kondus, V., Puzik, R., German, V., Panchenko, V., Yakhnenko, S. (2021). Improving the efficiency of the operating process of high specific speed torque-flow pumps by upgrading the flowing part design. *Journal of Process Mechanical Engineering*, Vol. 1741, 012023 https://doi.org/10.1088/1742-6596/1741/1/012023
10. Quan, H., Chai, Y., Li, R., Guo, J. (2019). Numerical simulation and experiment for study on internal flow pattern of vortex pump. *Engineering Computations*, Vol. 36, pp. 1579–1596. https://doi.org/10.1108/EC-09-2018-0420
11. Machalski, A., Skrypacz, J., Szulc, P., Blonski, D. (2021). Experimental and numerical research on influence of winglets arrangement on vortex pump performance. *Journal of Physics: Conference Series*, Vol. 1741, 12019. http://dx.doi.org/10.1088/1742-6596/1741/1/012019
12. Kovaliov, I., Ratushnyi, A., Dzafarov, T., Mandryka, A., Ignatiev, A. (2021). Predictive vision of development paths of pump technical systems. *Journal of Physics: Conference Series*, Vol. 1741, 012002. Retrieved from https://doi.org/10.1088/1742-6596/1741/1/012002
13. Andrenko, P., Grechka, I., Khovanskyy, S., Rogovyi, A., Svynarenko, M. (2021). Improving the technical level of hydraulic machines, hydraulic units and hydraulic devices using a definitive assessment criterion at the design stage. *Journal of Mechanical Engineering*, Vol. 18(3), pp. 57–76. https://doi.org/10.24191/jmeche.v18i3.15414
14. Andrenko, P., Rogovyi, A., Grechka, I., Khovanskyy, S., Svynarenko, M. (2021). Characteristics improvement of labyrinth screw pump using design modification in screw. *Journal of Physics: Conference Series*, Vol. 1741, 012024. https://doi.org/10.1088/1742-6596/1741/1/012024
15. Gusak, A.G., Krishtop, I.V., German, V.F., Baga, V.N. (2017). Increase of economy of torque flow pump with high specific speed. *IOP Conference Series: Materials Science and Engineering*, Vol. 233, 012004. https://doi.org/10.1088/1757-899X/233/1/012004
16. Krishtop, I. (2015). Creating the flowing part of the high energy-efficiency torque flow pump. *Eastern-European Journal of Enterprise Technologies*, Vol. 2(7(74)), pp. 31–37. https://doi.org/10.15587/1729-4061.2015.39934
17. Rogovyi, A., Korohodskyi, V., Neskorozhenyi, A., Hrechka, I., Khovanskyi, S. (2023). Reduction of granular material losses in a vortex chamber supercharger drainage channel. *In: Ivanov, V., Pavlenko, I., Liaposhchenko, O., Machado, J., Edl, M. (eds) Advances in Design, Simulation and Manufacturing V. DSMIE 2022. Lecture Notes in Mechanical Engineering*, pp. 218–226. Springer, Cham. https://doi.org/10.1007/978-3-031-06044-1_21
18. Kondus, V., Kalinichenko, P., Gusak, O. (2018). A method of designing of torque-flow pump impeller with curvilinear blade profile. *Eastern-European Journal of Enterprise Technologies*, Vol. 3(8(93)), pp. 29–35. https://doi.org/10.15587/1729-4061.2018.131159
19. Kondus, V., Kotenko A. (2017). Investigation of the impact of the geometric dimensions of the impeller on the torque flow pump characteristics. *Eastern-European Journal of Enterprise Technologies*, Vol. 1(4(88)), pp. 25–31. https://doi.org/10.15587/1729-4061.2017.107112
20. Dehghan, A., Shojaeefard, M., Roshanaei, M. (2024) Exploring a new criterion to determine the onset of cavitation in centrifugal pumps from energy-saving standpoint; experimental and numerical investigation. *Energy*, Vol. 293, 130681. https://doi.org/10.1016/j.energy.2024.130681
21. Dehnavi, E., Danlos, A., Solis, M., Kebdani, M., Bakir, F. (2024). Study on the pump cavitation characteristic through novel independent rotation of inducer and centrifugal impeller in co-rotation and counter-rotation modes. *Physics of Fluids*, Vol. 36(1), 015120. https://doi.org/10.1063/5.0182731
22. Panchenko, V., Ivchenko, A., Dynnyk, O., Drach, O. (2018). Increasing the technical level of a torque flow pump by changing the geometry of a flowing part. *Technology Audit and Production Reserves*, Vol. 3(1(41)), pp. 10–21. https://doi.org/10.15587/2312-8372.2018.135773
23. Gerlach, A., Thamsen, P., Lykholt-Ustrup, F. (2016). Experimental investigation on the performance of a vortex pump using winglets. *In: 16th International Symposium on Transport Phenomena and Dynamics of Rotating Machinery (ISROMAC 2016)*, hal-01518313v1. HAL Open Science, Honolulu, Hawaii.
24. Jung, D.-W., Seo, C.-W., Lim, Y.-C., Kim, S.-Y., Lee, S.-Y., Suh, H.-K. (2023). Analysis of flow characteristics of a debris filter in a condenser tube cleaning system. *Energies*, Vol. 16(11), 4472. https://doi.org/10.3390/en16114472
25. Gao, X., Shi, W., Zhang, D., Zhang, Q., Fang, B. (2014). Optimization design and test of vortex pump based on CFD orthogonal test. *Transactions of the Chinese Society for Agricultural Machinery*, Vol. 45(5), pp. 101–106. http://dx.doi.org/10.6041/j.issn.1000-1298.2014.05.016
26. Gerlach, A., Thamsen, P., Wulff, S., Jacobsen, C. (2017). Design parameters of vortex pumps: A meta-analysis of experimental studies. *Energies*, Vol. 10(1), 58. https://doi.org/10.3390/en10010058
27. Dehnavi, E., Solis, M., Danlos, A., Kebdani, M., Bakir, F. (2023). Improving The performance of an innovative centrifugal pump through the independent rotation of an inducer and centrifugal impeller speeds. *Energies*, Vol. 16(17), 6321. https://doi.org/10.3390/en16176321
28. Dehnavi, E., Bakir, F., Danlos, A., Kebdani, M. (2023). Numerical analysis of distance effect between inducer and centrifugal impeller in independent rotational turbopump in co-rotating and counter-rotating mode. *In: 15th European Conference on Turbomachinery Fluid Dynamics & Thermodynamics, ETC2023-23*, pp. 1–10. https://doi.org/10.29008/ETC2023-203

29. Bhattacharjee, P., Hussain, S.A.I., Dey, V. (2023). Failure mode and effects analysis for submersible pump component using proportionate risk assessment model: A case study in the power plant of Agartala. *International Journal of System Assurance Engineering and Management*, Vol. 14, pp. 1778–1798 https://doi.org/10.1007/s13198-023-01981-6
30. Makivskyi, O., Kondus, V., Pitel, J., Sotnyk, M., Andrusiak, V., Polkovnychenko, V., Musthai, M. (2024). The influence of the design features of the submersible pump rotor on the vibration reliability. *Journal of Engineering Sciences (Ukraine)*, Vol. 11(1), pp. D1–D9. https://doi.org/10.21272/jes.2024.11(1).d1
31. Schmirler, M., Netrebska, H. (2017). The design of axial shaftless pump. *EPJ Web of Conference*, Vol. 143, 02104. https://doi.org/10.1051/epjconf/201714302104
32. Zhang, H., Deng, C., Chang, C., You, H. (2022). Novel dual synergistic sealing ring design for a high-pressure pump – Part I. *Sealing Technology*, Vol. 2022(7). https://doi.org/10.12968/s1350-4789(22)70085-2
33. Zhang, H., Deng, C., Chang, C., You, H. (2022). Novel dual synergistic sealing ring design for a high-pressure pump – Part II. *Sealing Technology*, Vol. 2022(8). https://doi.org/10.12968/S1350-4789(22)70086-4
34. Panchenko, V., German, V., Ivchenko, O., Ryasnaya, O. (2021). Combined operating process of torque flow pump. *Journal of Physics: Conference Series*, Vol. 1741, 012011. https://doi.org/10.1088/1742-6596/1741/1/012022
35. Pavlenko, I. (2014). Static and dynamic analysis of the closing rotor balancing device of the multistage centrifugal pump. *Applied Mechanics and Materials*, Vol. 630, pp. 248–254. https://doi.org/10.4028/www.scientific.net/AMM.630.248
36. Chernobrova, A., Sotnik, M., Moloshnyi, O., Antonenko, S., Boiko, V. (2021) Influence of different volute casings theoretical methods design on pump working processes. *Journal of Physics: Conference Series*, Vol. 1741, 012014. https://doi.org/10.1088/1742-6596/1741/1/012014
37. Vaneev, S.M., Martsinkovskiy, V.S., Kulikov, A., Miroshnichenko, D.V., Bilyk, Y.I., Smolenko, D.V., Lazarenko A.D. (2021). Investigation of a turbogenerator based on the vortex expansion machine with a peripheral side channel. *Journal of Engineering Sciences (Ukraine)*, Vol. 8(1), pp. F11–F18. https://doi.org/10.21272/jes.2021.8(1).f2
38. Krishtop, I., German, V., Gusak, A., Lugova, S., Kochevsky, A. (2014). Numerical approach for simulation of fluid flow in torque flow pumps. *Applied Mechanics and Materials*, Vol. 630, pp. 43–51. https://doi.org/10.4028/www.scientific.net/amm.630.43
39. Rogovyi, A., Korohodsky, V., Medviedev, Y. (2021). Influence of Bingham fluid viscosity on energy performances of a vortex chamber pump. *Energy*, Vol. 218, 119432. https://doi.org/10.1016/j.energy.2020.119432